Optical Properties of the Alpha-Phase Alloys Ag-Zn and Ag-Cd†

E. L. Green
Navy Underwater Sound Laboratory, New London, Connecticut 06320
and
L. Muldawer
Temple University, Philadelphia, Pennsylvania 19122
(Received 16 February 1970)

Reflectance measurements at near-normal incidence have been performed on chemically polished, annealed, polycrystalline samples of Ag-Zn and Ag-Cd alloys. Data were obtained for Ag and Ag-Zn and Ag-Cd alloy samples with 2.5, 5.0, 10.0, 20.0, and 30.0% II *B* atom concentrations. The measurements were made with a precision of 2% of measured reflectance over a spectrum 1.2–13.5 eV at temperatures of 110, 295, and 400 °K. Dielectric constants were computed by the Kramers-Kronig method. Trends of the dielectric constants with either a Zn or Cd concentration are basically similar. The principal ϵ_2 peak of Ag at 4.0 eV moves to higher energies with an increase of II *B* atom concentration; however, a secondary peak, observed only in the alloys, moves to lower energies. Transitions probably occur in the alloys from the *d* band to the Fermi surface and also from the Fermi surface to the *s* band. The transition to the Fermi surface is dominant in Ag. Trends of the ϵ_2 peaks for alloys with a concentration of Zn or Cd follow an approximate free-electron model. Energy gaps in Ag deduced from the present data are in approximate agreement with the deductions of Berglund and Spicer from photoemission experiments. Marked differences exist between the Ag-Zn and the Ag-Cd alloys. The dilute (2.5%) Ag-Zn alloy has a distinctly sharper ϵ_2 edge than the corresponding Ag-Cd alloy. On the other hand, the low-energy absorption peak is seen first in the Ag-Cd alloy. These observations suggest that in the Ag-Zn alloy the additional electron contributed by the Zn tends to remain localized, whereas in the Ag-Cd alloy, it tends to contribute to the total number of free electrons and thereby increases the probability of transition to the *s* band. At 10% or higher concentrations, the optical characteristics are less sharply defined and the temperature effects are weaker for the Ag-Zn alloy than for the Ag-Cd alloy.

INTRODUCTION

The unique optical property of Ag is its very sharp interband edge in the near ultraviolet at 4.0 eV just at the point where free-electron absorption has fallen almost to zero. Consequently, the optical spectrum is separated into distinct intraband and interband regions. The 4.0-eV interband absorption edge in Ag is attributed usually to a transition from the *d* band to the Fermi surface in the [111] direction.[1,2] Optical measurements have provided the primary quantitative specification of the band gap. Photoemission studies,[3] however, indicate that transition in the region of 4.0 eV may occur from the Fermi surface to higher *s*-band levels as well as from the *d* band to the Fermi surface. Near the edge, the optical spectrum of Ag should show exceptional sensitivity to alloying and to temperature change. If nearly coincident interband transitions in this region involve free electrons either at initial or terminal states, then alloying Ag with either Zn or Cd should shift the Fermi surface to separate the two possible transitions. The temperature sensitivity of the alloy spectra is expected to decrease progressively with an increase of minority atom concentration and associated lattice disorder. This decrease in temperature sensitivity should be coupled with an over-all broadening of edge transitions in the optical absorption spectrum. Alloying may abruptly reduce the maximum of the energy-loss function for free electrons, which is calculable from optical measurements.[4] This decay would be associated with the vanishing of a well-defined near-zero absorption and the spreading of edges that are well defined in Ag at low temperature.

Studies of the optical properties of β-brass-type alloys as functions of temperature and composition have been reported by Muldawer[5] and Muldawer and Goldman.[6] Biondi and Rayne[7] have reported on the low-temperature absorptivity of α-Cu-Zn alloys. Recently Morgen and Lynch[8] have investigated the optical properties of dilute Ag-In alloys over a limited range (3.35–4.28 eV).

A systematic electronic band-structure study of the α phase of Ag-Zn and Ag-Cd alloys has not been performed. Amar and Johnson,[9] however, have studied the α phase of Cu-Zn alloys over a 0–30% range of Zn concentrations and have interpreted the optical properties of α-Cu-Zn alloys on the basis of their calculated bands.

The work described in this paper partially dupli-

cates the measurements made on Ag at room temperature by Ehrenreich and Philipp, [1] but over a more limited spectral range. The measurements reported here encompass Ag and its α-phase alloys with Cd and Zn at the following approximate concentrations of the IIB atom: 2.5, 5.0, 10.0, 20.0, 30.0%. Measurements were made at 110, 295, and 400 °K. The spectrum 1.2–13.5 eV was covered with emphasis on the interval 2.0–7.0 eV, where maximum temperature and composition effects were observed.

EXPERIMENTAL METHOD

A dual-beam vacuum reflectometer was constructed for the measurement of reflectance at 15° (near-normal) incidence on small polished metal samples in the wavelength range from 10 500 to less than 1000 Å. The reflectometer consists basically of a sample chamber and holder and incorporates cooling and heating elements, which may be attached to the 0.5-m Seya-Namioka–type monochromator. An argon discharge and a tungsten source are used in their appropriate spectral regions. Detectors are a sodium salicylate coated window used from 900 to 1800 Å, a quartz-windowed photomultiplier tube (EMI 6255S) used from 1800 to 6300 Å, and an infrared-sensitive tube used from 6300 to 10 500 Å. The beam from the monochromator is split; one-third of the light is diverted to a reference detector that is fixed in position and two-thirds impinges on the sample that reflects the light to the reflectance detector. After amplification, the ratio of the photocurrents is measured directly as a function of wavelength by a digital ratiometer. Precision of measurement in the tungsten region is 1.5% of measured reflectance. The precision in the near ultraviolet is comparable at stronger lines in the spectrum but otherwise is reduced somewhat by tube noise. Details of the unit and its operation may be found in a dissertation by Green. [10]

Precisely weighed quantities of the constituent metals were sealed under high vacuum in quartz tubes, melted, thoroughly mixed by continuous agitation in the furnace for 20 min, and then quenched in a water bath to form a homogeneous ingot. The ingot was cut into several sections from which reflectance samples were prepared. Material removed from the gaps between the sections was submitted to the U.S. Mint for an Ag assay, on the basis of which the composition in percent of Ag and IIB atoms was computed. The samples were finished to assure uniform fit in the reflectance sample holder and then sealed in evacuated quartz tubing and annealed for 24 h at high temperature (80 °C under the melting temperature). Preliminary mechanical surface finishing consisted of abrading the samples with 0, 2/0, 3/0, and 600 microcut paper. Final mechanical polishing was achieved with a gamal cloth impregnated with alumina.

Chemical polishing with chromic acid to remove the cold-worked surface layer produced by mechanical polishing essentially followed a procedure described for Ag. [11] We have found additionally that this solution is effective in producing a bright smooth surface on α-phase alloys of Ag-Zn and Ag-Cd. Immediately upon completion of the polishing operation the sample was mounted in the chamber, which was pumped down to under 5×10^{-6} Torr.

X-ray backreflection patterns were obtained from all samples following the optical measurements to confirm the effectiveness of the polishing method in removing the cold-worked layer.

DATA

The reflectance characteristic for Ag at 110 °K is shown for 1.2–15 eV in Fig. 1. From 2 to 7 eV, data on Ag and the Ag-Zn and Ag-Cd alloys were obtained at approximately 0.1-eV intervals. In the region of extreme temperature and composition sensitivity, data were obtained at 0.02-eV intervals. Beyond 7 eV, measurements were made at strong spectral lines only; Ag and the Ag-Zn and Ag-Cd alloys were essentially indistinguishable in this region. Experimental data curves obtained for each specimen below 7.0 eV were extended to 7.6 eV in such a manner as to join smoothly with a vacuum-ultraviolet reflectance characteristic that was fitted to experimental data points obtained over the full range of compositions and temperatures. Data for all samples were normalized to 0.91 at low energy by multiplying the measured reflectance in each case by a constant factor independent of energy. The 0.91 reflectance is a representative number characterizing these samples. The three temperature reflectance characteristics for Ag are

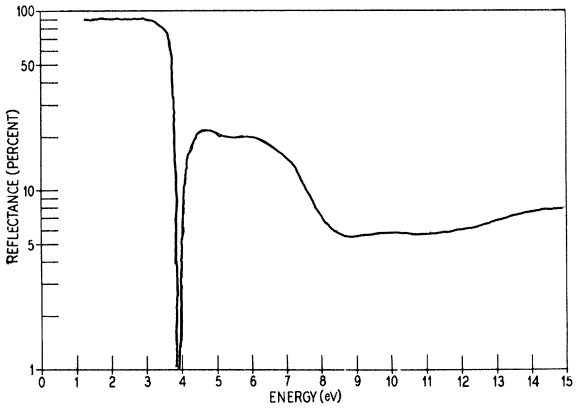

FIG. 1. Reflectance of Ag at 110 °K.

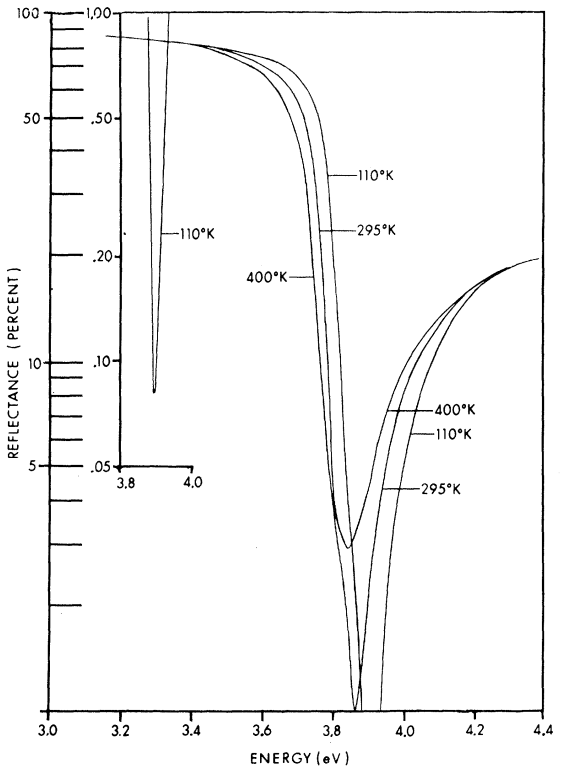

FIG. 2. Reflectance of Ag at 110, 295, and 400 °K.

shown on an expanded energy scale (3.0–4.4 eV) in Fig. 2. The trend of the Ag reflectance data with temperature is consistent with earlier observations.[12] Representative data for all the alloys are illustrated in the range to 7.0 eV by the $Ag_{95}Cd_5$ curves of Fig. 3. The superimposed dashed curve represents 110 °K silver. In the more dilute alloys, with 2.5–5.0% IIB element concentration, a trend toward the Ag characteristic is observed as temperature decreases. The trend in reflectance characteristics with an increase in the IIB element concentration is qualitatively similar to the trend for an increase of temperature. The reflectance minimum in the dilute Ag-Zn alloys, especially at 2.5%, is deeper than that of the corresponding Ag-Cd alloys. On the other hand, for higher IIB concentrations, the Ag-Cd characteristics have sharper edges and show greater detail than the corresponding Ag-Zn curves. Reflectance was measured as a function of temperature on all samples through 20% IIB concentration. At 20% concentration, variation of reflectance with temperature was small: it was not measurable in the case of $Ag_{80}Zn_{20}$ and was barely detectable for $Ag_{80}Cd_{20}$. Temperature variation in $Ag_{70}Cd_{30}$ was not measurable. Only room-temperature data were taken for the 30% Zn alloy. In the low-energy (high-reflectance) region the measurement precision (1.5%) was insufficient to reveal temperature- or composition-dependent differences.

A thin dielectric film may exist on the surface of the polished metal since final sample preparation is carried out with chemicals in the atmosphere. The evidence that variable films at least are not a problem in these data is the high degree of reproducibility of the reflectance functions, especially near the minima. Another indication is the good reproducibility of measured reflectance at intense lines in the vacuum ultraviolet. The calculations to ascertain the effect of films are straightforward but lengthy.[13] Lynch[14] made machine calculations on the effect of small thicknesses (up to 30 Å) of a film of index 1.75 on the reflectivity of Ag near the minimum. His results suggest films on our samples may have an optical thickness no greater than about 10 Å.

The most serious source of error in this experiment is probably scattering of light. The scattering from grain boundaries and etched regions of the chemically polished sample is readily apparent by visual inspection. Additional scattering may occur even from apparently smoothly polished areas. A theory of the scattering process by Porteus,[15] which is probably applicable to these specimens, is available. Scattering from the etched regions may be characterized as a process involving elements

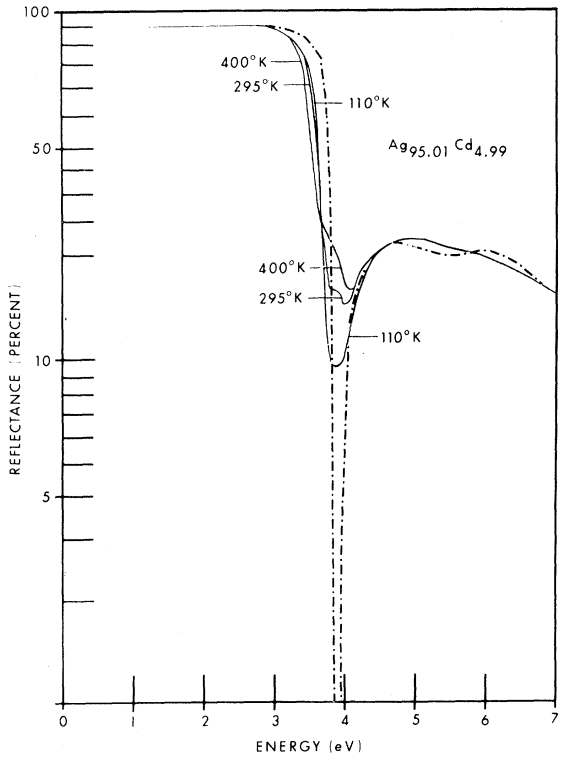

FIG. 3. Reflectance of $Ag_{95.01}$ $Cd_{4.99}$.

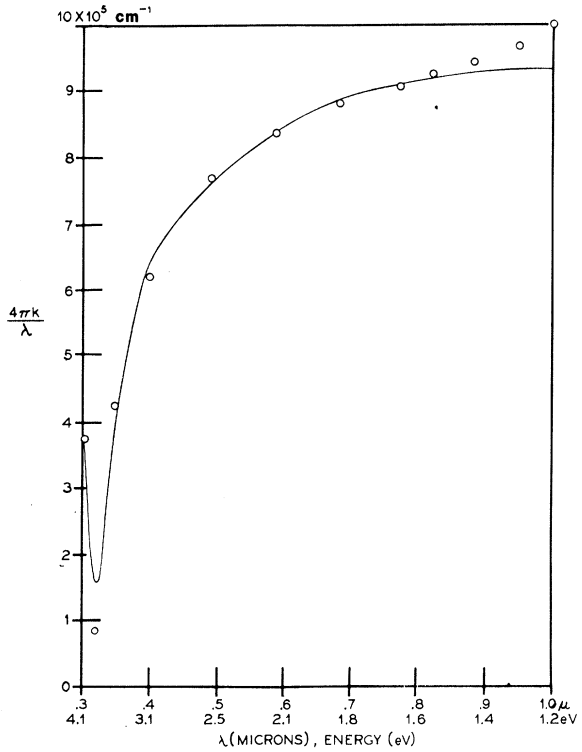

FIG. 4. $4\pi k/\lambda$ for Ag (curve from Schulz's data; points from present data).

that are larger than the wavelength of light. In terms of the rms roughness σ defined by Porteus, σ/λ is greater than 1 in the etched region. In this region scattering is incoherent, that is, diffuse and independent of the wavelength of light. Very little of the scattered light will impinge on the detector because of its small acceptance angle. Over the smooth part of the surface, wavelength-sensitive scattering may occur. In this region rms roughness is much less than the wavelength of light, but a roughness of even 0.01 of the wavelength of light may measurably reduce reflectance. The error attributable to roughness could become increasingly serious at short wavelengths. Measurements on vacuum-deposited Ag have been reported recently for the region 1000–2000 Å.[16] These reflectances are somewhat higher in the region of 2000 Å than values reported by Ehrenreich and Philipp[1] for electrolytically polished Ag or for the reflectances reported here on chemically polished Ag. The greater surface roughness of the bulk samples is a possible source of the reflectance difference. Fortunately, the differences between film and bulk measurements are not so large as to affect seriously the conclusions to be drawn from this experiment.

The 0.91 low-energy reflectance has no general physical significance. It is probable that variable losses occur as a consequence of scattering from grain boundaries and etched regions of the chemically polished sample. The 0.91 figure implies an unreasonably high degree of absorption, which is certainly not intrinsic to the bulk material. Alternative renormalization procedures for long wavelengths using (a) reflectance measurements at room temperature from smooth vacuum-deposited Ag films[17] or (b) reflectance derived from measurements of n and k of Ag at long wavelength[18] would not have been appropriate for these alloys. Since no trend of reflectance at low energy against composition could be observed on these chemically polished samples, the data for Ag and the Ag-Zn and Ag-Cd alloys were renormalized to 0.99 prior to calculation of the dielectric constants. It has been shown for the α-Cu-Zn alloys that the variation of low-temperature residual absorptivity from Cu to 30% Zn concentrations is less than 2%. This is a significant difference, but would not be measurable by the experimental procedure employed in the present study.

KRAMERS-KRONIG ANALYSIS

The Kramers-Kronig method was used to compute dielectric constants and related quantities on the basis of normal-incidence reflectance data. Experimental data curves provided input from 1.2 to 13.5 eV (from 10 500 to 918 Å). The published data of Ehrenreich and Philipp[1] for Ag were the basis of an extrapolation used from 13.5 to 23.0 eV for all the calculations. The computer program provides for two extrapolations beyond the limits of the input data. Thus, on the low-energy side, the constant low-energy reflectance was extended from 1.0 to 0. On the high-energy side, another constant may be chosen from 23.0 eV to infinity; computations, in fact, were performed for three independent high-energy extrapolations.

Computations were performed on all data for the 0.91 low-energy normalization representative of this experiment and also for 0.99 renormalization at low energy. The dielectric constants and energy-loss functions, represented graphically, are based upon the 0.99 renormalization, with extrapolations at 0.99 to zero energy and from 23.0 eV to infinity at 0.008. The high-energy extrapolation was chosen by trial and error to yield a coefficient $4\pi k/\lambda$ which from 3000 to 9600 Å matches very closely the results of Schulz[18] that are based on direct transmission measurements through films of Ag of increasing thickness (Fig. 4). The ultraviolet reflectance spectrum from about 6 to 13.5 eV is, within the limits of this experiment, not dependent on composition or temperature. It will be assumed that the spectrum beyond 13.5 (representative of higher-energy transitions) is also insensitive to composition and temperature. Accord-

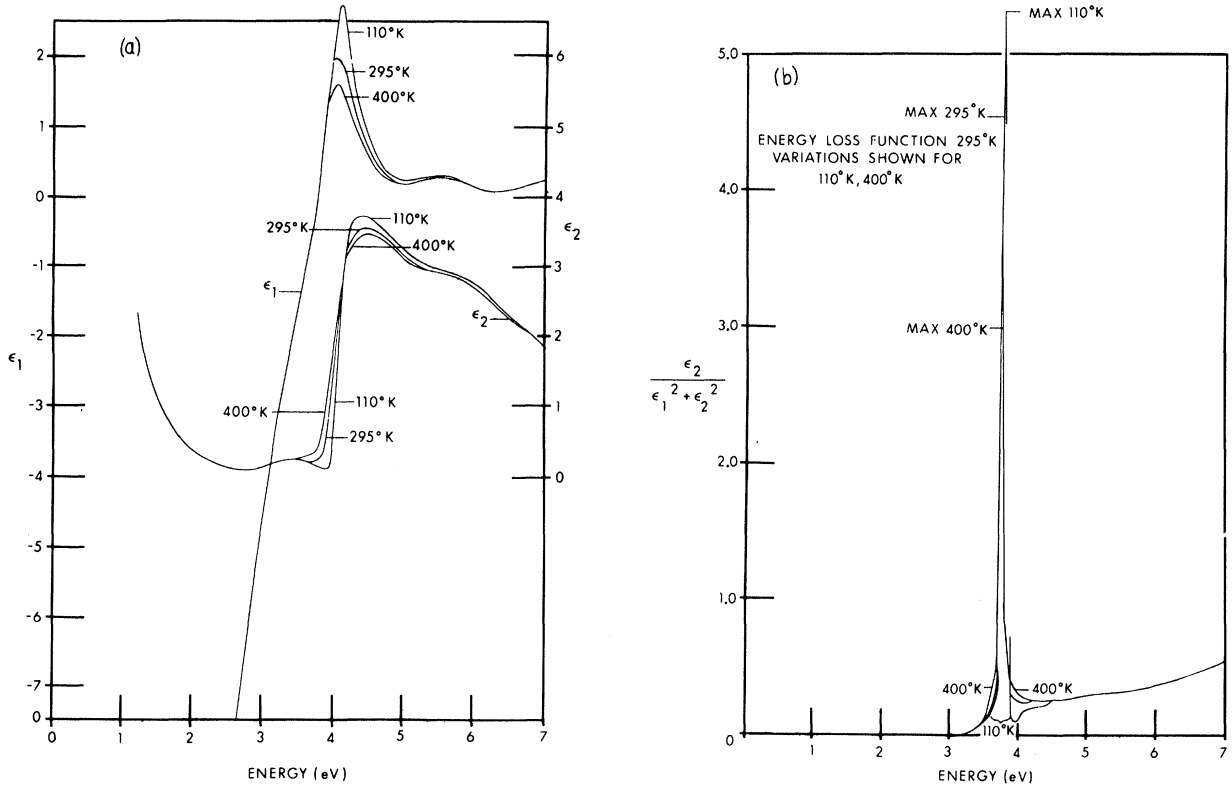

FIG. 5. Dielectric constants and energy-loss function of Ag.

ingly, the high-energy extrapolation determined for Ag has been used for all the alloys. The long-wavelength renormalization for all compositions and the extrapolation from 1 eV to 0 were set at 0.99. Any changes in the computed dielectric constants and related functions upon variation of composition or temperature are attributable, therefore, solely to the differences in the measured reflectance functions and not to the choice of extrapolation constants. Computations have been performed for the entire range, 1.0–23.0 eV of input data. Results for the dielectric constants are, however, plotted only in the narrower region where variations between the samples are significant. Beyond 7.0 eV, as might be anticipated, the computed dielectric constants are almost independent of composition.

Although, in principle, the absorption may be divided into two components, free-electron absorption and interband absorption, the data of this experiment relate principally to interband effects, i.e., in all cases the free-electron absorption is small at the onset of the interband absorption. In the interband region the forms of the calculated functions are essentially independent of the extrapolations. The computed dielectric constants and energy-loss functions at 110, 295, and 400 °K for

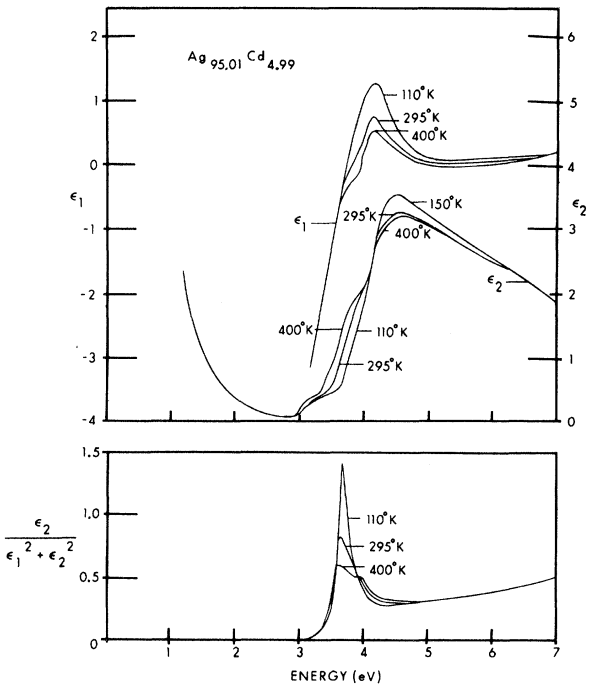

FIG. 6. Dielectric constants and energy-loss function for $Ag_{95.01}$ $Cd_{4.99}$.

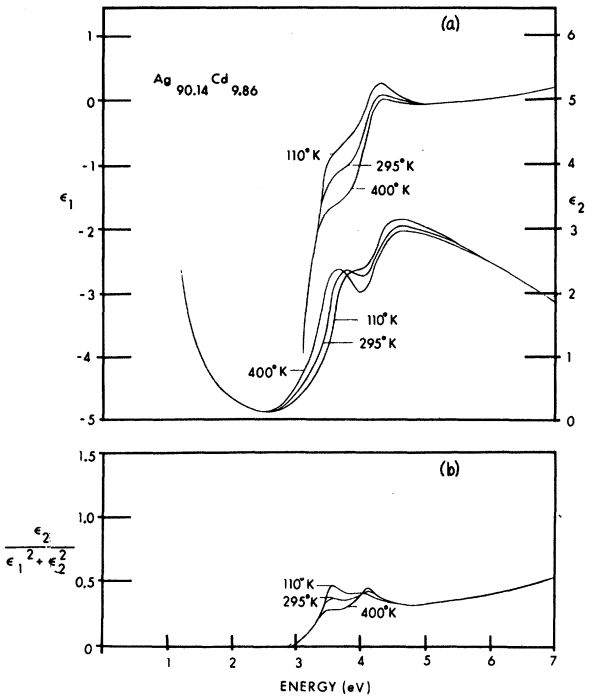

FIG. 7. Dielectric constants and energy-loss function for $Ag_{90.14}$ $Cd_{9.86}$.

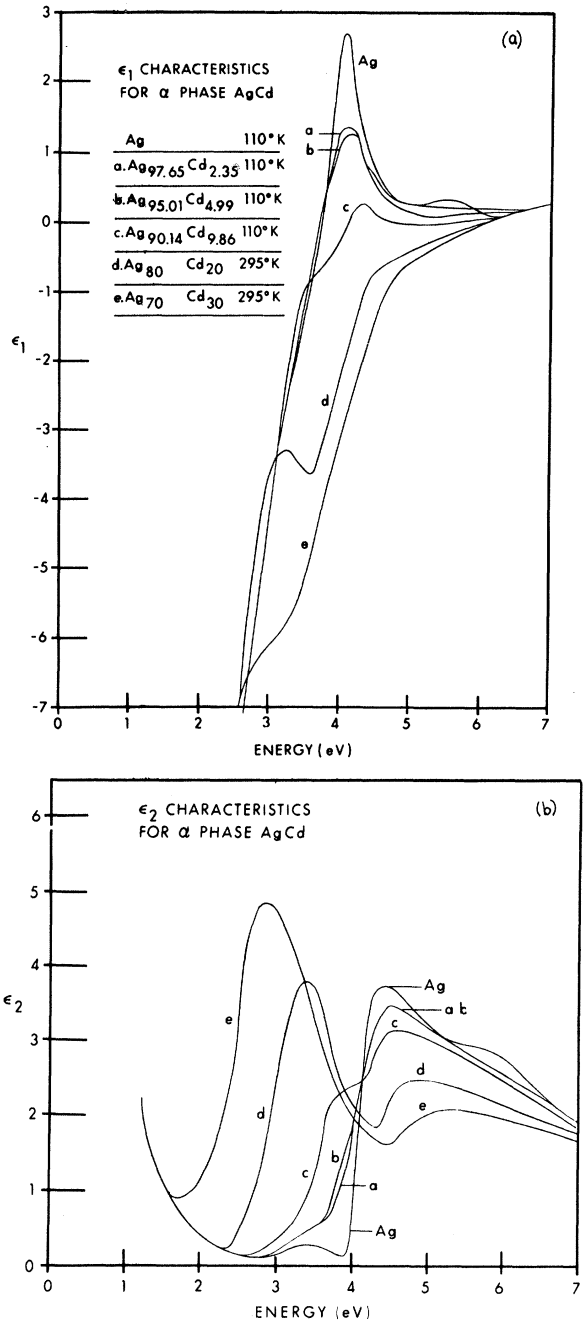

FIG. 8. Dielectric constants of Ag-Cd.

Ag are shown in Figs. 5(a) and 5(b). For the alloys $Ag_{95}Cd_5$ and $Ag_{90}Cd_{10}$ computed functions are shown in Figs. 6 and 7. Dielectric constants for Ag and the Ag-Cd alloys through 30% Cd are shown in Figs. 8(a) and 8(b). The dielectric constants are shown for Ag and the Ag-Zn alloys in Figs. 9(a) and 9(b) In Table I certain calculated values are tabulated for two representative cases, Ag at low temperature and $Ag_{95.01}Cd_{4.99}$ at high temperature. The coefficients $4\pi k/\lambda$ are shown for a low energy, 2.1 eV. The next column gives the energy (in eV) at which ϵ_1 crosses zero. In the next three columns the respective maximum values of ϵ_1, ϵ_2, and $\epsilon_2/(\epsilon_1^2+\epsilon_2^2)$ are listed. Calculations are tabulated for both 0.99 and 0.91 normalization. The three rows of values listed for each specimen correspond to three high-energy extrapolations. The first row shows the result of integrating from 0 to 23 eV and omitting a high-energy extrapolation. The following two rows give results for two other high-energy extrapolations, 0.002 and 0.008. As has been stated, the 0.99 and 0.008 combination is the basis for all of the curves showing computed dielectric constants and related functions. We note immediately that the tabulated functions are not strongly affected by the large change from 0.99 to 0.91 normalization, although the artificially low reflectance results in a large pseudoabsorption which is superimposed on the interband absorption. Small variations in reflectance near 0.99, such as those associated with the experimental error in the visible region, evidently would not greatly affect these quantities. Substantial variation in the low-energy normalization or, in fact, in fitting the curve to the data near the onset of interband absorption washes out detail in the low-energy tail of the interband ϵ_2, but it does not significantly affect ϵ_2 and related functions in most of the interband region. The tabulated functions are very sensitive to the high-energy extrapolation with one

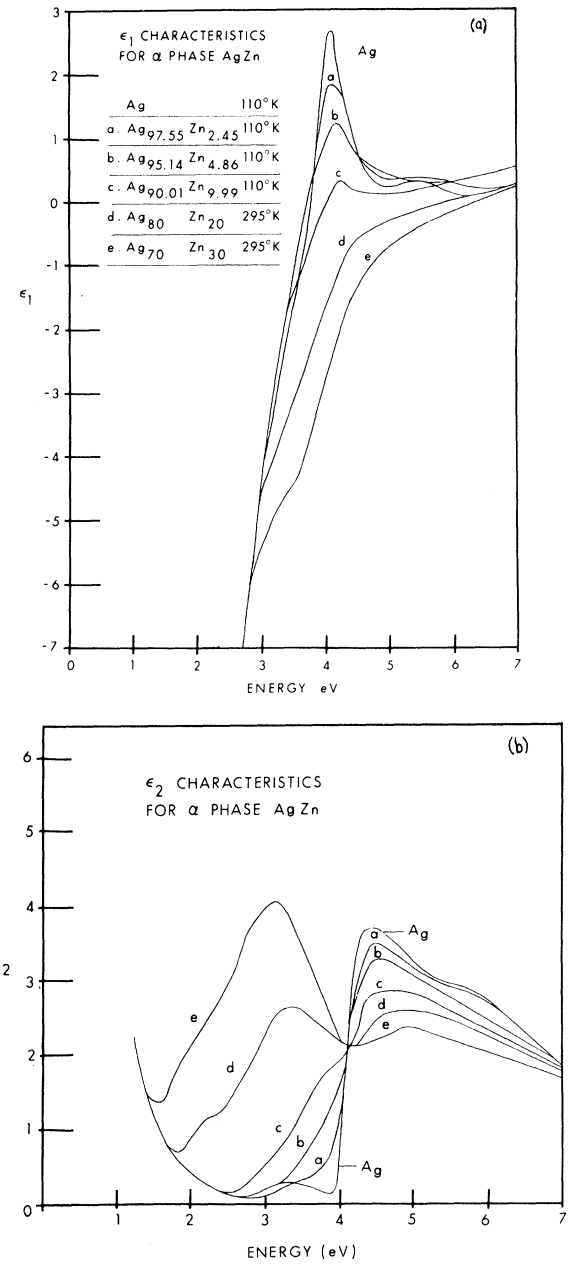

FIG. 9. Dielectric constants of Ag-Zn.

interesting exception. Readily seen is the essential invariance of the point at which ϵ_1 first passes through zero. The invariance of the zero of ϵ_1 has been noted in calculations for β-Cu-Zn alloys.[19]

The accuracy of the derived ϵ_1 and ϵ_2 functions is dependent firstly on the precision of the normal-incidence measurements and secondly on the validity of the normalization and extrapolation procedures. In the vicinity of the interband absorption, where reflectance changes are measured with relatively high precision, the computed n and k values, the dielectric constants, and the related quantities are reasonably consistent with directly measured values for evaporated films of silver.[20] The results are consistent also with the data of Ehrenreich and Philipp.[1] No direct measurements have been carried out for the α-phase alloys of Ag over a substantial energy range.

The energy at which ϵ_1 first passes through zero is significant primarily because of its intimate relationship to the energy-loss function for a charged particle. In Figs. 8(a) and 9(b) it may be noted that 10% and higher IIB element concentrations show a definite trend of the zero of ϵ_1 toward higher energy. From the equation expressing ϵ_1 as a function of ϵ_2 the following condition for $\epsilon_1 = 0$ may be derived[21]:

$$\frac{1}{\pi}\int_0^\infty \frac{d\epsilon_2}{d\omega}\ln\left(\left|\frac{1}{\omega^2-\omega_1^2}\right|\right)d\omega = -1\ , \qquad (1)$$

where ω_1 is the frequency for which $\epsilon_1 = 0$. From Eq. (1) it follows that a decrease in slope of ϵ_2 on the high-frequency side of the zero of ϵ_1 could cause an increase of the energy at which ϵ_1 passes passes through zero. A simple shift of the interband transition edge to higher energy with no change in shape also would shift the zero of ϵ_1 to higher energy; a shift of the lower edge to lower energy would decrease the zero energy. Thus, the zero of ϵ_1 follows the trend with energy of the principal ϵ_2 edge as the IIB atom concentration increases. In principle, both ϵ_2 and ϵ_1 can be separated into in-

TABLE I. Representative computed values.

Representative case	High-energy extrapolation	$\left(\frac{4\pi k}{\lambda}\right)$ at 2.1 eV		Energy (eV), where $\epsilon_1=0$		$(\epsilon_1)_{max}$		$(\epsilon_2)_{max}$		$\left(\frac{\epsilon_2}{\epsilon_1^2+\epsilon_2^2}\right)_{max}$	
		0.99	0.91	0.99	0.91	0.99	0.91	0.99	0.91	0.99	0.91
Ag (110 °K)	None	11.60	11.06	3.79	3.79	3.94	3.72	4.52	3.96	3.99	2.78
	0.008	8.27	8.01	3.79	3.79	2.71	2.63	3.74	3.49	5.54	5.29
	0.002	7.63	7.41	3.79	3.79	3.32	2.29	3.34	3.17	5.74	6.40
$Ag_{95.01}Cd_{4.99}$ (400 °K)	None	12.02	11.44	3.82	3.74	2.23	2.33	4.86	4.43	0.406	0.428
	0.008	8.49	8.22	3.94	3.90	0.539	0.667	3.22	3.08	0.601	0.635
	0.002	7.82	7.59	3.98	3.94	0.342	0.463	2.79	2.70	0.675	0.712

terband and intraband components. In the context of the free-electron theory, substitution of IIB atoms for Ag atoms increases the number of free electrons per unit volume and thus also increased the free-electron plasma frequency $\omega_p \sim N^{1/2}$, where N is the number of free electrons. On this basis, an increase of the zero of ϵ_1 with IIB concentration is to be expected. It is noteworthy, however, that the zero remains essentially unchanged in the dilute (up to 5.0% IIB concentration) alloys even though the ϵ_2 peak is shifting slightly. Inspection of the ϵ_2 characteristics shows a gradually increasing low-frequency "tail," which may be related to relaxation processes in the disordered lattice. The tail probably contributes to the integral Eq. (1) in such a manner as to compensate for the increases in the interband transition energy and in the free-electron plasma energy.

INTERPRETATION OF DATA

Interband Absorption in Ag and Ag-Zn and Ag-Cd

The data of this paper relate principally to interband effects, since in all cases the free-electron (intraband) absorption is small at the onset of interband absorption. An examination of the low-temperature ϵ_2 characteristic for Ag [Fig. 5(a)] reveals three distinct absorption regions in the interval 2–7 eV. The small rise near 3.50 eV is followed by a distinct minimum at 3.88 eV and a precipitous rise to a maximum at 4.4 eV. In the vicinity of 5.6 eV there is a distinct change in the slope of the characteristic.

The ϵ_2 characteristic for Ag in the interval 3.5–4.5 eV is very similar to that of Joos and Klopfer,[20] which also shows the small peak near 3.5 eV. Garfunkel *et al.*[22] have confirmed the peak in piezo reflectivity measurements. Stanford *et al.*[23] and Schnatterly[24] suggested recently that structure below 3.9 eV may be attributable to a surface plasom mode coupling to the radiation field via surface roughness.

The main peak in Ag at 4.4 eV is attributed by Ehrenreich and Philipp[1] to a direct transition from the d band to the Fermi surface, L_3 to L_2'. Our data support the view that the transition from the d band to the Fermi surface (L_3-L_2') is dominant over the other possible transition having approximately the same energy, that is, the Fermi surface to the s band (L_2'-L_1). Berglund and Spicer[3] on the basis of photoemission data also found transitions from the d band to be dominant, but they could not agree that they were direct transitions.

The change in slope of the ϵ_2 characteristic at 5.6 eV was also observed by Ehrenreich and Philipp,[1] who associated the structure with the transition (X_5-X_4').

The more dilute alloys of Ag with Zn and Cd are similar to Ag in over-all form of the ϵ_2 characteristic and in the display of marked temperature effects (Figs. 6 and 7). There is a notable similarity, especially at low temperature, between the 2.5% Ag-Zn and Ag [Fig. 9(b)]. The principal difference is the vanishing in this alloy of the distinct 3.9-eV minimum. When the 2.5% Ag-Zn alloy is compared with the 2.5% Ag-Cd alloy, the latter is less like Ag. The ϵ_2 function of the 2.5% Ag-Cd has a secondary absorption peak, which is temperature dependent, on the low-energy side of the principal peak. At 5.0% concentration, we note (Fig. 6) a distinct subsidiary absorption maximum on the low-energy side of the principal maximum. In the corresponding 5.0% Zn alloy this splitting is not observed. With 10.0% Zn concentration, the splitting is observed at all temperatures. The 10.0% Zn alloy shows a plateau on the low-energy side of the principal ϵ_2 maximum. Energy-loss functions peak sharply at low temperatures in the 2.5 and 5.0% alloys, but are weak at higher concentrations of Zn or Cd. The effects of increase of temperature at a given concentration and of increase of concentration of IIB atoms at a given temperature are analogous. Increase of temperature from 110 to 400 °K is equivalent to a small increase in concentration of the IIB atoms. Structure of the reflectance functions and the dielectric constants are more like Ag in the dilute Ag-Zn alloys than in the corresponding Ag-Cd alloys. With higher concentrations the structure is more distinct in the Ag-Cd alloys. The low-energy ϵ_2 peaks in the 20 and 30% Cd alloys are higher than in the Zn alloys and the half-widths of absorption are narrower. Temperature effects are very prominent in the 10.0% Ag-Cd alloy and, on the other hand, just detectable in the 10.0% Ag-Zn alloy. Temperature variations of reflectance are not detectable at larger Zn concentrations but are just detectable over the interval 110–400 °K in the 20% Cd alloy. The close analogy between temperature and composition effects suggests a common origin, namely, changes in the distribution of electrons in energy states near the Fermi level.

Free-Electron Model

The dielectric constants of the α-phase alloys [Figs. 8(a) and 8(b) for Ag-Cd and Figs. 9(a) and 9(b) for Ag-Zn] deviate from the Ag values progressively with IIB atom concentration. In both systems of alloys, a second principal peak of ϵ_2 is observed, and this peak moves toward lower energy as the original Ag peak moves toward higher energy. Morgan and Lynch[8] have observed a similar trend in dilute (less than 5% In) Ag-In alloys. This second peak clearly is not related to the minor maxi-

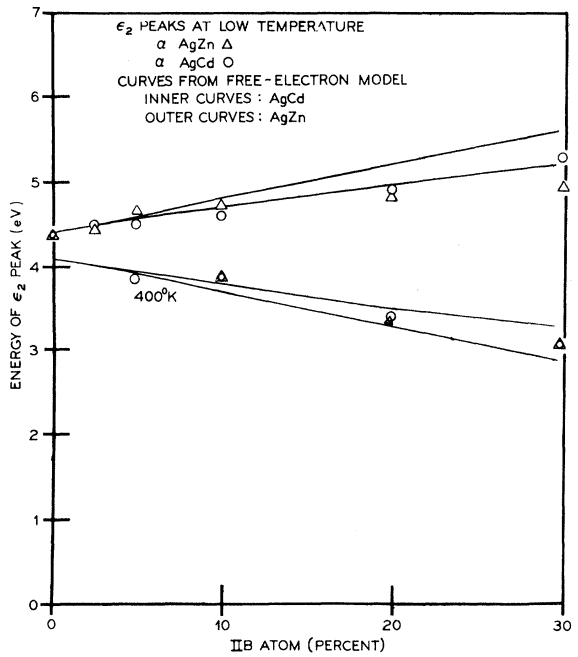

FIG. 10. ϵ_2 peaks versus IIB atom concentration.

mum observed in Ag at approximately 3.5 eV. If the high-energy peak were associated with transitions principally from d bands to the Fermi distribution (L_3-L_2') and the low-energy peak with transitions principally from the vicinity of the Fermi surface to the s band (L_2'-L_1), then the trends might be described fairly well by a progressive displacement of the Fermi surface consequent on the increase in free-electron concentration. Figure 10 shows the location of ϵ_2 peaks in α Ag-Zn and Ag-Cd alloys as functions of IIB atom concentration. The curves on which the data points are superimposed are derived from the fixed-rigid-band, or free-electron, model, i.e., on the basis of the approximation that a Fermi sphere is expanding in an empty lattice as electrons are added, one additional electron for each IIB atom that displaces a Ag atom. The calculation determines only the slope of the curves.

The absolute energy scale has been located empirically. In particular the position of the curves for the low-energy peaks is based necessarily on data for 10.0, 20.0, and 30.0% alloys. The data point for 5.0% Cd at 400 °K is shown. In computing the free-electron curves, we have taken into account the fact that the lattice expands with an increase in Cd concentration and contracts with an increase in Zn concentration. Both the high- and low-energy peaks observed in the alloys converge with small IIB concentration into the single peak of Ag. The variation of heights of the peaks is attributable partially to the $1/E^2$ factor relating the dielectric constant to the transition matrix element. (E is the energy of the transition.) The data indicate strongly that the dominant transition in Ag is that from the d band to the Fermi surface. The low-energy peak observed in the Ag-Cd alloys and in 10.0, 20.0, and 30.0% Ag-Zn must be much weaker in Ag. A high joint density of states exists in Ag and the alloys for the transition from the d band (L_3) to a region above the Fermi surface near L_2'. The transition from the Fermi surface to L_1 probably exists in Ag; in the alloys the joint density of states for this transition increases with IIB atom concentration. Extrapolating ϵ_2 peaks in the alloys to zero concentration (Fig. 10), one observes that the Fermi surface in Ag is less than 4.4 eV above L_3 and less than 4.1 eV below L_1.

The energy gaps for Ag in the L direction deduced from the present data are summarized below and in Fig. 11:

$$L_1 - E_F = 3.88\,\text{eV} \approx 3.9\,\text{eV}, \quad L_1 - L_2' = 4.1\,\text{eV},$$

$$E_F - L_3 = 4.4\,\text{eV}, \quad E_F - L_2' = 0.2\,\text{eV}.$$

Berglund and Spicer on the basis of photoemission data deduced the following differences, in close agreement with our results:

$$L_1 - L_2' = 4.2\,\text{eV}, \quad E_F - L_2' = 0.3\,\text{eV}.$$

They also found a peak in state density about 0.3 eV wide located 4.1 eV below the Fermi surface, which may be associated with the transition from L_3 to E_F.

With an increase of Cd or Zn (free-electron) concentration the ϵ_2 peaks follow the change in energy of the Fermi surface. So also is the temperature

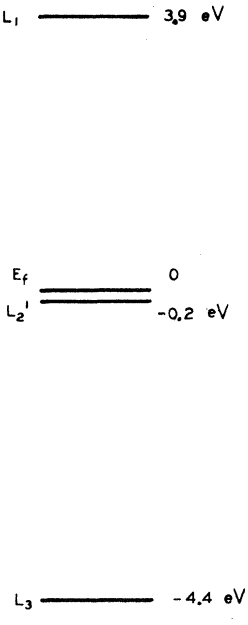

FIG. 11. Energy levels in [111] direction referred to Fermi level.

sensitivity of the low-energy ϵ_2 peaks associated with spread of the Fermi surface in accordance with the Fermi distribution function. The temperature data for Ag-Cd alloys suggest that states exist just above the Fermi surface from which transitions may occur to the s band. Raising the temperature causes a significant number of these normally empty states to be occupied. Note, for example, that at 110 °K the probability of finding an electron at 0.35 eV above the Fermi level is 0.025; at 400 °K the probability is about 0.25. The thermal shift in electron density above the Fermi level for the 290 °C temperature change is approximately equivalent to an increase of 2.5% in Zn or Cd concentration.

Both an increase in temperature and an increase in IIB atom concentration will spread the Fermi surface. In the disordered lattice this spread is a consequence of the degeneracy of energy states, $E(k)$. The sharpness of the Fermi edge in the k space at low temperature in a disordered lattice may be measured approximately by the change in reflectance and dielectric constants consequent upon heating the specimen. For example, if the low-temperature edge of ϵ_2 pertaining to a transition involving the Fermi electrons is blurred such that the effect of a temperature rise is barely detectable, then the change in the Fermi distribution that results from the temperature rise is approximately equal to the intrinsic spread of the Fermi edge. Lattice vibrations also spread the ϵ_2 edge as temperature rises in a manner equivalent to intrinsic lattice disorder by decreasing free-electron relaxation time. But the data of this experiment definitely indicate that the Fermi distribution is the dominant factor causing temperature changes in the optical properties in the Cd alloys and, for lack of any comparable alternative, also in the other alloys and in Ag. Joos and Klopfer[20] also believed that the change in the Fermi distribution function could account for the changes with temperature that they observed in the optical properties of Ag.

Difference between Ag-Zn and Ag-Cd Alloys

The marked differences between the Ag-Zn and Ag-Cd alloys have been noted. The dilute (2.5%) Zn alloy possesses a distinctly sharper edge than the corresponding Cd alloy. On the other hand, the dilute Cd alloy has a weak low-energy absorption peak at high temperature. For the 5.0% alloy the high-temperature splitting is clear in the Ag-Cd and is nonexistent in the Ag-Zn. The free-electron model accounts for the shift of transition energies $(L_3\text{-}L_2')$ and $(L_2'\text{-}L_1)$ over the entire measured range of Cd concentration. But beyond 10% Zn both the Fermi surface and L_1 are closer to the d bands than the simple model predicts. This tendency in α-phase Ag-Zn, that is, a shift downward of the conduction band with respect to d bands, is analogous to the shift in α-Cu-Zn deduced by Lettington[25] from his analysis of the data of Biondi and Rayne[7] and calculated by Amar and Johnson[9] from a theoretical model.

The similarity of its optical characteristics to Ag suggests that in dilute Ag-Zn the additional electron contributed by a Zn atom tends to remain localized. This tighter binding is consistent with comparative chemical properties of cadmium and zinc. Cadmium is more active than zinc and is more easily dissolved in weak acids. The additional electron contributed by a Cd atom tends to contribute to the total number of electrons, thereby raising the Fermi level to place electrons in normally vacant energy states, where they may contribute to the transition from Fermi level to s band. At 10% or higher concentrations of Zn, the Ag-Zn band structure is less sharply defined than that of the corresponding Cd alloys, whether measured by slope of the ϵ_2 edges or by comparative temperature effects. It is possible that the same stronger atomic field which binds the electron to the Zn core where the IIB atoms are relatively far apart tends to disrupt the periodic field at higher concentrations.

ACKNOWLEDGMENTS

The authors gratefully acknowledge helpful conversations with K. Johnson on the band structure of solids and the assistance of G. Kessler in the construction of the apparatus and of M.O. Fein in the preparation of samples.

---

†Paper based on a 1965 Ph.D. dissertation by E. L. Green, who was sponsored by U.S. Army, Frankford Arsenal, Philadelphia, Pa. Work performed at Temple University laboratory facilities, funded in part by the Atomic Energy Commission.

[1]H. Ehrenreich and H. R. Philipp, Phys. Rev. 128, 1622 (1962).

[2]B. R. Cooper, H. Ehrenreich, and H. R. Philipp, Phys. Rev. 138, A494 (1965).

[3]C. N. Berglund and W. E. Spicer, Phys. Rev. 136, A1030 (1964); 136, A1044 (1964).

[4]P. Nozières and D. Pines, Phys. Rev. 113, 1254 (1959).

[5]L. Muldawer, Phys. Rev. 127, 1551 (1962).

[6]L. Muldawer and H. Goldman, in *Proceedings of the International Colloquium, Paris*, edited by F. Abeles

(North-Holland, Amsterdam, 1966), pp. 574–585.
[7]M. A. Biondi and J. A. Rayne, Phys. Rev. 115, 1522 (1959).
[8]R. M. Morgan and D. W. Lynch, Phys. Rev. 172, 628 (1968).
[9]H. Amar and K. Johnson, in Ref. 6, pp. 586–598.
[10]E. L. Green, thesis, Temple University, 1965 (unpublished).
[11]H. Levinstein and W. H. Robinson, Trans. Met. Soc. AIME 224, 1992 (1962).
[12]J. V. Pennington, Phys. Rev. 39, 953 (1950).
[13]O. S. Heavens, *Optical Properties of Thin Solid Films* (Academic, New York, 1965).
[14]D. W. Lynch (private communication).
[15]J. O. Porteus, J. Opt. Soc. Am. 53, 1394 (1963).
[16]L. R. Canfield and G. Hass, J. Opt. Soc. Am. 55, 61 (1965).
[17]J. M. Bennett and E. J. Ashley, Appl. Opt. 4, 221 (1965).
[18]L. G. Schulz, Phil. Mag. Suppl. 6, 102 (1957).
[19]K. Johnson and R. Esposito, J. Opt. Soc. Am. 54, 474 (1964).
[20]G. Joos and A. Klopfer, Z. Physik 138, 251 (1954).
[21]F. Stern, *Solid State Physics*, edited by F. Seitz and D. Trumbull (Academic, New York, 1963), Vol. 15, p. 332, Eq. 19.1(a).
[22]M. Garfunkel, J. J. Tiemann, and W. E. Engeler, Phys. Rev. 155, 1046 (1967).
[23]J. L. Stanford, H. E. Bennett, J. M. Bennett, and E. J. Ashley, Bull. Am. Phys. Soc. 13, 989 (1968).
[24]S. E. Schnatterly, Bull. Am. Phys. Soc. 13, 989 (1968).
[25]A. H. Lettington, Phil. Mag. 11, 863 (1965).

PHYSICAL REVIEW B VOLUME 2, NUMBER 2 15 JULY 1970

Isothermal and Isolated Susceptibilities for a Nonlinear Refractive Index

M. Takatsuji

Hitachi Central Research Laboratory, Kokubunji, Tokyo, Japan

(Received 29 December 1969)

Using a canonical-transformation method, a formal expression for the isothermal polarization induced by an arbitrarily time-varying field is obtained which includes the population change due to the energy shift which is proportional to the field intensity. The result is applied to the static linear susceptibility and nonlinear refractive index induced by an intense laser beam. It is shown for the latter that the lowest- (third-) order isolated susceptibility of an isotropic medium is a lower bound for the isothermal susceptibility if both the polarizations and frequencies of the laser beam and the probe light are the same.

I. INTRODUCTION

The concepts of the isothermal and isolated susceptibilities of electric or magnetic media are well established. In the isothermal process, the system is in thermal contact with the heat bath and maintains its temperature constant at all times when the field is applied, while in the isolated process the system was in thermal contact with the heat bath at the infinite past which was then isolated from its surroundings. The field is applied very slowly (adiabatically in Ehrenfest's sense), and the isolated motion of the system obeys the Liouville equation. Quantum mechanically, the population of a given energy level must be held constant for the isolated process, while for the isothermal process the population change is possible. The difference of the two susceptibilities arises from this fact.

The quantum-statistical formulations of both the isolated susceptibility for a time-varying field[1] and the static isothermal susceptibility[2] have been accomplished to every order in the applied field. However, there seems to be no general formulation of the isothermal susceptibility for an arbitrarily time-varying field. The main purpose of the present paper is to deal with this problem by a quantum-statistical method.

Performing a canonical transformation on the Liouville equation, the rapidly oscillating part of the Hamiltonian is eliminated. The density matrix for the isolated system is then driven by a time-independent Hamiltonian at time t, when the system is again brought into contact with the heat bath so that it is represented by a new equilibrium density matrix. It is found in Sec. II that the isothermal expectation value of an operator is obtained by replacing the equilibrium density matrix at the infinite past by the new one in the expression for the isolated expectation value of the operator. In Sec. III, the result is applied to the well-known problem of static linear susceptibilities. Those for the nonlinear refractive index induced by an intense laser beam are discussed in Sec. IV.